RSC Advances

PAPER

View Article Online
View Journal | View Issue

Cite this: *RSC Adv.*, 2016, **6**, 5223

Competitive removal of Cd(II) and Pb(II) by biochars produced from water hyacinths: performance and mechanism†

Yang Ding,[ab] Yunguo Liu,*[ab] Shaobo Liu,*[cd] Zhongwu Li,[ab] Xiaofei Tan,[ab] Xixian Huang,[ab] Guangming Zeng,[ab] Yaoyu Zhou,[ab] Bohong Zheng[c] and Xiaoxi Cai[ab]

Received 9th December 2015
Accepted 23rd December 2015

DOI: 10.1039/c5ra26248h

www.rsc.org/advances

Three biochars converted from water hyacinth biomass at 300, 450, and 600 °C were used to investigate the adsorption properties of Cd^{2+} and Pb^{2+}. In addition, the competitive adsorption mechanisms between Cd^{2+} and Pb^{2+} were also conducted. Adsorption kinetics and isotherms indicated that the maximum adsorption capacity of Pb^{2+} was larger than that of Cd^{2+}, and the adsorption process in the mixed solutions of two heavy metals (Cd^{2+} and Pb^{2+}) was more favorable for Pb^{2+}. Further investigation about the characterization of biochars demonstrated that cation exchange, surface complexation, cation–π interaction and precipitation were the main mechanisms responsible for the heavy metal removal. In this study, competitive adsorption may also be explained by these mechanisms. These results are useful for the application of biochars in selective adsorption and in practical wastewater treatment.

1. Introduction

Heavy metals may cause serious environmental pollution and threaten public health due to their toxic and non-biodegradable nature.[1] They are mainly discharged from human activities such as metal plating, mining and paper industries. Cadmium, lead, chromium, and nickel are the most common heavy metal pollutants which could pose a risk to human health even at micro-concentrations.[2,3] Therefore, some cost-effective methods need to be developed to remove heavy metal compounds from waste water. Most of the traditional water treatment technologies have disadvantages of either low efficiency or overspend. Biosorbents have attracted wide attention in recent years because of the universality of materials and the high efficiency of adsorption.

Although activated carbon (AC) has been used to remove various pollutants,[4,5] the costs of the AC application in the treatment is higher than that of biochar. Moreover, biochar is characterized by high affinity for contaminants in literatures,[6,7] thus it potentially may be an alternative for AC. Biochar is a form of carbon black produced through the thermal pyrolysis process of biomass under inert atmosphere conditions. There are many types of biomass such as wood waste, crop residues, organic wastes, which have been utilized as feedstock for biochar production.[8–10] Biochar has been widely applied for removing toxic substances from waste water. For instance, Dong, *et al.* found that biochar produced from sugar beet tailing had a strong affinity for Cr(VI) with the sorption capacity of 123 mg g^{-1}.[11] Similarly, Gan, *et al.* indicated that biochar produced from sugarcane bagasse had a good adsorption capacity for Cr(VI).[12] Compared to biochar derived from hardwood, corn straw biochar had a good adsorption capacity for both Zn(II) and Cu(II).[13] In addition, Kim, *et al.* demonstrated that the Cd removal capacity of biochar produced from a giant Miscanthus increased with the increasing of pyrolytic temperatures.[14]

However, pollution of multiple heavy metals is commonly existed in practical wastewater. Therefore, it is inevitable to study the adsorption properties and mechanisms of biochar in a mixed solution of several heavy metals. Chen, *et al.* reported that Cu(II) would compete with Zn(II) for binding sites at Cu(II) and Zn(II) concentrations $\geq$ 1.0 mM.[13] In our previous study, Pb(II) adsorption at high concentrations would be inhibited by the competition from phenol in binary system, but phenol adsorption was scarcely affected due to the directly phenol molecular adsorption pattern.[15] Little competition occurred between Pb and atrazine for sorption on dairy-manure derived biochar, while strong competition was observed on a commercial activated carbon.[16] As two kinds of common heavy metals pollutants, further studies focused on the mechanisms of

[a]*College of Environmental Science and Engineering, Hunan University, Changsha 410082, PR China. E-mail: hnliuyunguo@163.com; Fax: +86 731 88822829; Tel: +86 731 88649208*

[b]*Key Laboratory of Environmental Biology and Pollution Control (Hunan University), Ministry of Education, Changsha 410082, PR China*

[c]*School of Architecture and Art Central South University, Central South University, Changsha 410082, P. R. China. E-mail: liushaobo23@aliyun.com; Fax: +86 731 88710171; Tel: +86 731 88830923*

[d]*School of Metallurgy and Environmental, Central South University, Changsha 410083, P.R. China*

† Electronic supplementary information (ESI) available. See DOI: 10.1039/c5ra26248h

competitive adsorption between Cd(II) and Pb(II) are also needed to be conducted.

In Xiangjiang river basin, seasonal outbreak of water hyacinth is favored by the subtropical monsoon climate. Water hyacinth has been considered as aggressive invasive species by IUCN (the International Union for Conservation of Nature). The aggressive invasion of water hyacinth could pose threats to native ecosystem, including depleting the water of oxygen and destroying the native biodiversity. The conversation of water hyacinth into biochar and then application in the treatment of pollutants may be environment friendly.

In this study, water hyacinths were used to prepare biochars *via* slow pyrolysis at different pyrolysis temperatures ranged from 300 to 600 °C. The resulted biochars were applied to adsorb contaminants from aqueous solutions contained Cd(II), Pb(II), and the mixture of Cd(II) and Pb(II). The specific objectives of this study were to (i) examine Cd and Pb sorption isotherms and kinetics onto biochars; (ii) investigate the underlying mechanisms governing Cd^{2+} and Pb^{2+} adsorption by biochars; (iii) explore the properties of competitive adsorption between Cd^{2+} and Pb^{2+}; (iv) understand the influence of three biochars on Cd^{2+} and Pb^{2+} adsorption and determine the optimal pyrolysis temperature.

2. Materials and methods

2.1. Biochar preparation

Water hyacinths (WHs) were collected in Changsha, Hunan province, China. WHs were washed with ultrapure water three times to remove the attached dust, and then dried at 90 °C for more than 24 h. The biochar samples (BCs) used in this study were produced by slowly pyrolyzing the dried WHs in a lab-scale pyrolyzer (SK-G08123K, China) under N_2 at 300, 450, and 600 °C for 2 h. The reactor was heated with a heating rate of 5 °C min^{-1}. These biochars were cooled to room temperature under a nitrogen condition. BCs were ground through a 0.15 mm sieve for this experiment. The biochars obtained at different temperatures are referred to as BC300, BC450, and BC600, respectively. Finally, they were stored in desiccators before use.

2.2. Biochar characterization

The elements of BCs were analyzed by an ESCALAB 250Xi X-ray Photoelectron Spectrometer (XPS) (Thermo Fisher, USA). Brunauer, Emmett and Teller (BET) surface area was determined using a gas sorption analyzer (Quantachrome Quadrasorb SI, USA) and the total pore volume was examined from the N_2 adsorption–desorption isotherms. Functional groups of biochar's surface were measured by a Fourier transform infra-red spectrophotometer (FTIR) (Nicolet Magna-IR 750, USA). A scanning electron microscopy (SEM) (JSM-7001F, Japan) was used to analyze the surface features of BCs before and after adsorption. The pH of the point of zero charge (pH_{pzc}) was measured using Electroacoustic Spectrometer (ZEN3600 Zetasizer, UK) by adding 0.1 g BCs to solution with pH range from 1.0 to 10.0. Inductively coupled plasma-atomic emission spectrometry (ICP-AES) (Baird PS-6, USA) was selected to detect the concentrations of released cations from BC450.

2.3. Batch adsorption and desorption experiments

Ultrapure water with a resistivity of 18.25 MΩ cm^{-1} was used in this study. Cd^{2+} and Pb^{2+} stock solution (1000 mg L^{-1}) were prepared by dissolving analytical grade 2.7442 g cadmium nitrate tetrahydrate ($Cd(NO_3)_2 \cdot 4H_2O$) and analytical reagent 1.5985 g lead nitrate ($Pb(NO_3)_2$) into 1000 mL ultrapure water, respectively. In single system, these stock solutions were diluted to 50–900 mg L^{-1}. In binary system, the concentrations of Cd^{2+} and Pb^{2+} (0.25–2 mmol L^{-1}) were prepared.

The impact of pH on biochar adsorption was examined by adjusting the initial Cd^{2+} solutions (100 mg L^{-1}) ranging from 2.0 to 7.0, as well as Pb^{2+} solutions (100 mg L^{-1}) ranging from 2.0 to 5.0, considering the formation of precipitates under high solution pH (Cd > 7; Pb > 5). The initial pH of different Cd^{2+}, Pb^{2+}, and the mixture solutions were both adjusted to 5 by adding 1 M NaOH or 1 M HCl. Sorption kinetic was conducted by adding 0.1 g biochar (BC300, BC450, and BC600) to 50 mL of the 100 mg L^{-1} solutions. These suspensions were shaken at 140 rpm at 30 °C for the designated time periods. Experiments for adsorption isotherms were conducted at the initial concentrations of solutions (50, 100, 150, 200, 250, 400, 500, and 900 mg L^{-1}) and the shaking period of 24 h. In order to studying the competitive adsorption mechanisms between Cd^{2+} and Pb^{2+}, 0.25 or 0.5 mmol L^{-1} Pb^{2+} (Cd^{2+}) was added into the prepared Cd^{2+} (Pb^{2+}) solutions. Thermodynamic data were obtained at the temperature of 25, 30, and 40 °C based on the experiments of adsorption isotherms. The influence of background ionic strength on adsorption was studied at appropriate pH with the addition of different concentrations of NaCl (0, 0.005, 0.01, 0.05, 0.1, 0.2, 0.5, and 1.0 mol L^{-1}). BC450 with 0.1 g was added into each solution, and suspensions were shaken at 140 rpm under 30 °C for 24 h. The amount of cations (K, Ca, Na and Mg) released from BC450 after Cd or Pb sorption was determined. Aliquots of biochar were added to Cd or Pb solution (500 mg L^{-1}) and ultrapure water (control), respectively, at a 1 : 20 ratio followed by agitation for 24 h. The concentrations of K, Ca, Na and Mg in the filtrate were determined using ICP-AES. The net cations released were calculated by subtracting cations released in control.

Desorption experiment included the following steps: 0.1 g biochar (BC300, BC450, BC600) was added into 50 mL of 500 mg L^{-1} heavy metal solution and shaken at 140 rpm and 30 °C for 24 h. Then the suspensions were filtered (0.22 μm filter) and biochars were rinsed three times with ultrapure water. Biochars which have been used to sorb heavy metals were then added into the solution of HCl (0.5 mol L^{-1}) and shaken for 24 h.

2.4. Heavy metal analysis

All experiments suspensions were filtrated, and then the residual concentration of each heavy metal in the filtrate (0.22 μm filter) were determined using atomic absorption spectrometer (AAS) (AAnalyst700, Perkin-Elmer, US). The adsorption

capacity (Q_e) and the adsorption percentage (S, %) were calculated according to:

$$Q_e = \frac{V(C_0 - C_e)}{M} \quad (1)$$

$$S = \frac{C_0 - C_e}{C_0} \times 100 \quad (2)$$

where: C_0 and C_e are the initial and equilibrium concentration of heavy metals (mg L^{-1}), V is the volume of adsorption solution (mL), and M is the weight of biochar (g).

3. Results and discussion

3.1. Characteristics of biochars

The product yields of BC300, BC450 and BC600 were 67.6%, 49.5% and 34.4%, respectively. The loss in yield was increased with the increase of pyrolysis temperature. The surface chemical elements of biochar before and after adsorption were determined by X-ray photoelectron spectroscopy (XPS). From the XPS survey spectra, the main elements of pristine biochar were carbon (64.29%), oxygen (24.3%), potassium (9.46%), nitrogen (1.53%), phosphorus (0.42%) and biochar after adsorption were carbon (77.72%), oxygen (17.29%), nitrogen (2%), phosphorus (0.42%), lead (2.2%), cadmium (0.36%), potassium (not detected because of the extremely low content). As shown in Fig. 1, the binding energy of carbon functional groups changed in some extent after adsorption, indicating the important role of carbon functional groups in adsorption mechanisms. In addition, four peaks were observed in the C 1s XPS spectra, including C–C (284.8 eV), C–O (286.5 eV), C=O (288.4 eV), O–C=O (290.3 eV). The XPS survey spectra (Fig. 2) demonstrated that two new peaks appeared at the binding energy of 139.7 eV and 406.3 eV after biochar sorption, which presented the existence of Pb 4f and Cd 3d, respectively. Moreover, this adsorption process was favourable to the removal of Pb because the peak area of Pb was higher than that of Cd.

Scanning electron microscopy (SEM) images revealed that the surface morphologies of biochar before and after adsorption had some obvious changes. As shown in the Fig. S1a,† the surface of biochar before heavy metal adsorption was extremely rough and the pore structure of pristine biochar was highly inhomogeneous. However, Fig. S1b† and 2 showed that a layer of materials was covered on the surface of biochar, which may attribute to the adsorption of Pb and Cd onto biochar. Moreover, some flaky particles were observed on the surface of biochar after adsorption, and the possible explanation was that the precipitation of heavy metals was formed on the surface of biochar. Therefore, multiple adsorption mechanisms should be responsible for the Pb and Cd removal.

The BET characteristics of BC450 were presented in Table S1.† The BET surface area of the BC450 was 51.15 m^2 g^{-1} and pore volume was 0.06667 cm^3 g^{-1}, which were higher than many other biochars reported in studies. The surface area and pore volume of the biochar in the present study were larger than those of sugarcane bagasse.[10] The pore volume of the biochar was greater than these of the biochars produced from wood and bark of pine oak.[17]

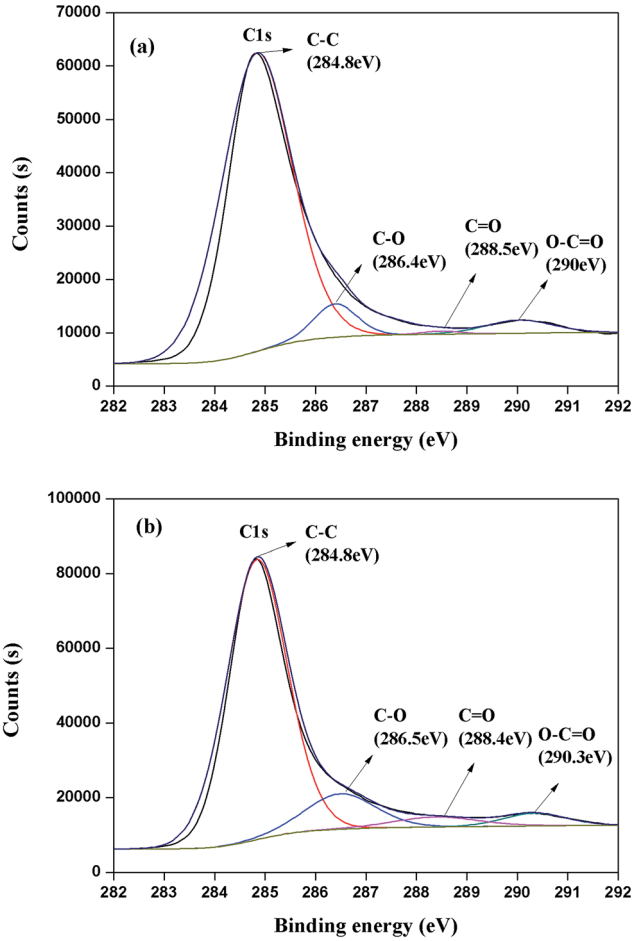

Fig. 1 C 1s XPS spectra of BC450 (a) before and (b) after adsorption.

The FTIR spectra of BC300, BC450 and BC600 were shown in Fig. 3. Different wavenumbers were observed in the same functional groups of three biochars. Characteristic peak of BC450 at 3417.3 cm^{-1} was due to the stretching vibration of

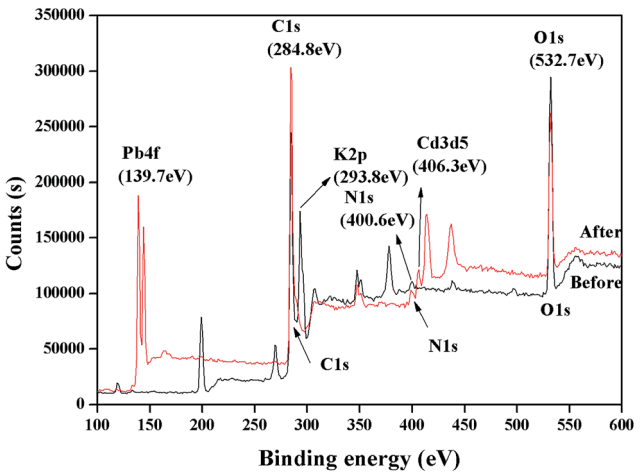

Fig. 2 XPS survey spectra of BC450 before and after adsorption.

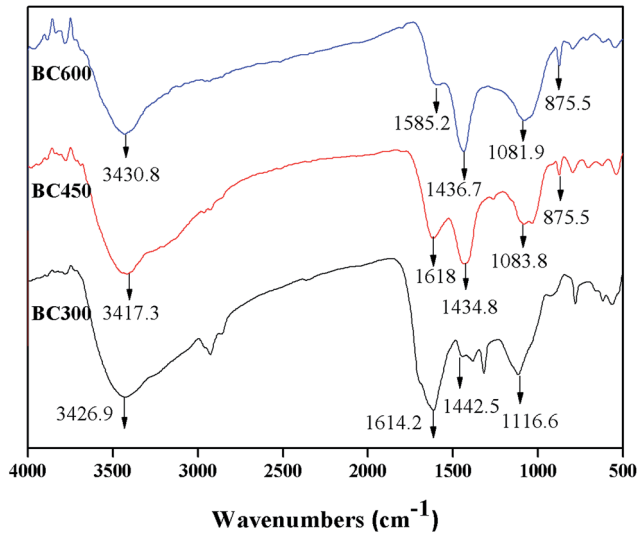

Fig. 3 FTIR spectra of BC300, BC450 and BC600.

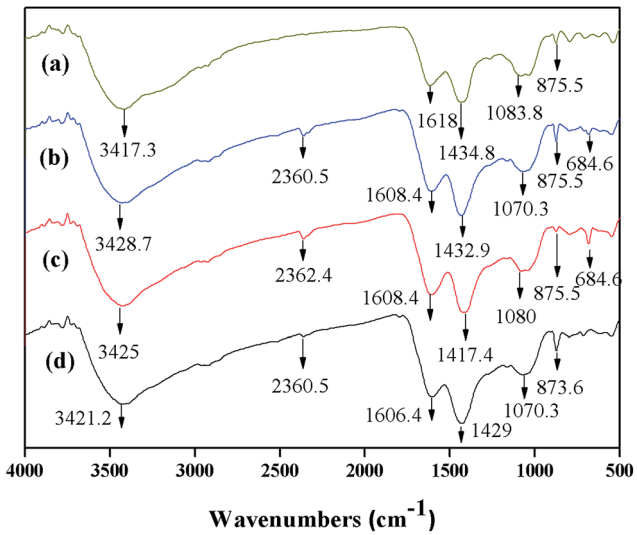

Fig. 4 FTIR spectra of BC450 (a) before and after (b) the mixture, (c) Pb and (d) Cd adsorption.

–OH groups. The band at 1618 cm^{-1} was related to the stretching vibration of –OH deformation of water and C=O stretching vibration of the carbonyl from the carboxyl group in biochars.[18] The peak at 1434.8 cm^{-1} was connected with COO– groups and the broad band near at 1083.8 cm^{-1} may be attributed to the C–O bending vibration or the band of the out-of-plane bending for carbonates (CO_3^{2-}) or to the P–O bond of phosphate in biochars,[19,20] which was consistent with the high surface P contents of BC450 indicated by the XPS results. Moreover, there was a new band at 875.5 cm^{-1} when the pyrolysis temperature was above 450 °C, which was related to γ-CH furan.[21] These heterocyclic compounds were a weak cation–π binder. Furthermore, the peak at 3417.3 cm^{-1} and 1618 cm^{-1} became weak because of the reduction of oxygen-containing functional groups especially the disappearance of hydroxyl.

The FTIR spectra of BC450 before and after Cd, Pb and the mixture adsorption were presented in Fig. 4. The band at 3417.3 cm^{-1} shifted to the higher wavenumbers after adsorption. Those peaks, such as C=O, –OH, and COO–, shifted slightly to the lower wavenumbers. After adsorption, a new peak at around 2360 cm^{-1} was found, which could be assigned to C≡C in-line deformation vibration or carbon dioxide.[18] These results indicated that the main adsorption mechanism was highly related to the functional groups of biochar.

3.2. Effect of pH on the adsorption of heavy metals

The pH is a major factor affecting adsorption of heavy metals on aqueous solutions. The adsorption capacity of Cd(II) and Pb(II) increased with the increase of system pH (Fig. 5a). The zero point of zeta potential (pH_{zpc}) was 2.3 for BC450 (Fig. 5b). When the solution pH < pH_{zpc}, the biochar surface contained positive charge because of the protonation of biochar's hydrated surface. Therefore, a strong electrostatic repulsion occurred between positive charged biochar surface and cationic Pb(II) or Cd(II) ions, which could be responsible for the lowest adsorption capacity at pH 2.0. Moreover, abundant of H^+ in this solution could compete with Pb^{2+} and Cd^{2+} for available

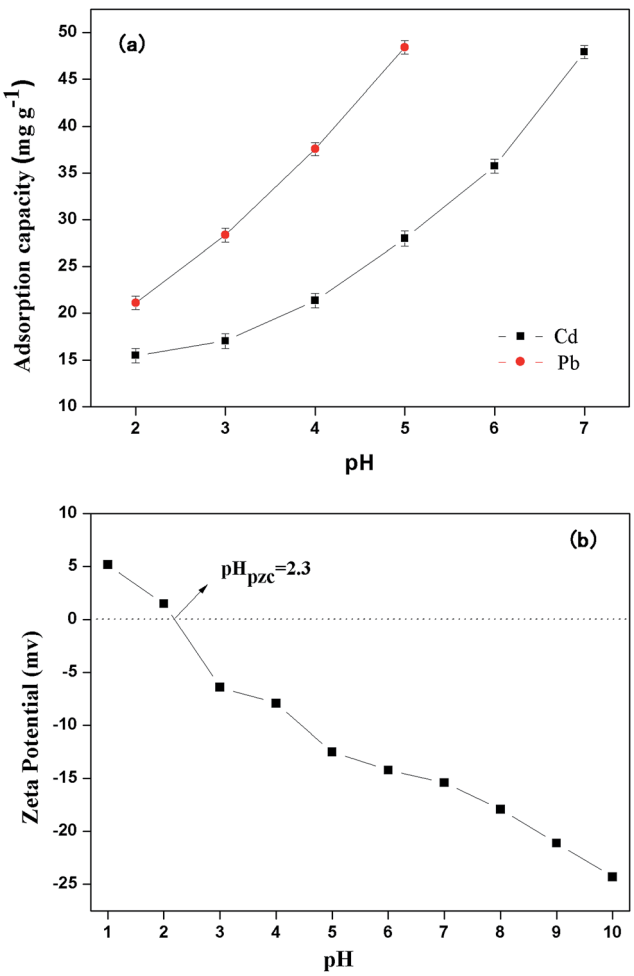

Fig. 5 (a) Effect of initial solution pH values on Cd and Pb adsorption by BC450. (b) Zeta potentials of BC450 at different solution pH values.

adsorption sites on biochar. However, biochar became negative charge due to the deprotonation of adsorbent's hydrated surface when pH > pH_{zpc}. The capacity of electrostatic attraction increased with the increasing of pH value, indicating a positive correlation between adsorbate and adsorbent. Considering the formation of precipitate of high concentration Pb and Cd (*e.g.*, 1 g L^{-1}) under a relative high pH value, pH 5.0 was chosen for Cd, Pb and the mixture of Pb and Cd.

3.3. Kinetic studies

The kinetic of heavy metals sorption on biochars was simulated using pseudo first order kinetic model and pseudo second order kinetic model.[22] These equations can be expressed as follows:

$$q_t = q_e\left(1 - e^{-k_1 t}\right) \quad (3)$$

$$q_t = \frac{k_2 q_e^2 t}{1 + k_2 q_e t} \quad (4)$$

where k_1 (min^{-1}) and k_2 (g mg^{-1} min^{-1}) are the rate constant of the pseudo first order and the pseudo second order, q_t and q_e are the adsorption amounts (mg g^{-1}) at time t and equilibrium, respectively.

The correlation coefficient (R^2) of the pseudo-second-order model was higher than that of the pseudo-first-order model (Table 1), indicating the experimental data fitted better to pseudo-second-order model. As shown in Fig. 6, both Cd(II) and Pb(II) adsorption were rapidly happened within the beginning 6 h, and adsorption capacities were 41.05 mg g^{-1} and 43.2 mg g^{-1}, respectively. Furthermore, the values of q_e calculated from pseudo-second-order model ($R^2 = 0.94$) were more fitted in the experimental q_e value, indicating that the mechanism of theses adsorption process depended on the rate limited chemisorption, such as complexation and precipitation.[23]

3.4. Adsorption isotherms

Langmuir and Freundlich adsorption models were used to fit the heavy metals adsorption isotherm data.

The Langmuir model:

$$q_e = \frac{q_{max} K_L C_e}{1 + K_L C_e} \quad (5)$$

The Freundlich model:

$$q_e = K_F C_e^{1/n} \quad (6)$$

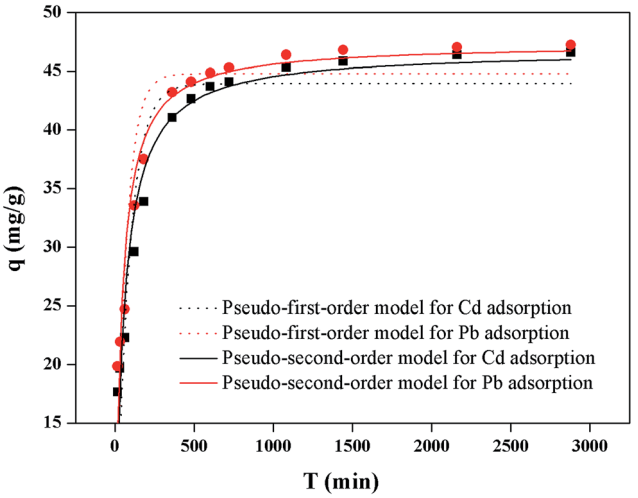

Fig. 6 Pseudo-first-order sorption kinetics and pseudo-second-order sorption kinetics for Cd and Pb adsorption onto BC450 in single system (initial heavy metals concentration: 100 mg L^{-1}; pH: 5.0; reaction temperature: 30 °C).

where C_e is the equilibrium concentration (mg L^{-1}), q_e (mg g^{-1}) is the amount of heavy metals adsorbed at equilibrium, q_{max} (mg g^{-1}) is the maximum adsorption capacity of the solute. The K_L (L mg^{-1}) and K_F ((mg g^{-1}) (mg $L^{-1})^{-n}$) are the adsorption coefficients of Langmuir model and Freundlich model, respectively. The n is the Freundlich linearity constant related to the surface site heterogeneity.

The relative parameters calculated from Langmuir model and Freundlich model were listed in Table 2. It obviously demonstrated that all biochars' correlation coefficient (R^2) values of Langmuir model at three temperatures were higher than those of Freundlich model, which suggested that these adsorption data of heavy metals onto biochars fitted Langmuir model better than Freundlich model.

The Cd^{2+} and Pb^{2+} adsorption isotherms on different biochars at three temperatures demonstrated that the amount of heavy metals adsorbed onto biochars (BC300, BC450, and BC600) increased with the increasing of reaction temperature (25, 30, and 40 °C). Langmuir isotherm and Freundlich isotherm for the adsorption of Cd and Pb on biochars at 30 °C were presented in Fig. 7. Table S3† presented the comparison of the maximum Cd(II) or Pb(II) adsorption capacity of various adsorbents in the previous study. As seen, the prepared water hyacinth biochars maintained much higher Cd(II) and Pb(II) removal performance than many other adsorbent materials reported in the literature.

Table 1 Pseudo-first-order and pseudo-second-order model parameters for Cd(II) and Pb(II) adsorption on BC450 at 30 °C

	Pseudo-first-order			Pseudo-second-order		
Pollutants	k_1 (min^{-1})	q_e (mg g^{-1})	R^2	k_2 (g mg^{-1} min^{-1})	q_e (mg g^{-1})	R^2
Cd(II)	0.01235	43.94	0.84	0.0004233	46.79	0.94
Pb(II)	0.01629	44.78	0.82	0.0005578	47.33	0.94

Table 2 Langmuir and Freundlich isotherms parameters for Cd^{2+} and Pb^{2+} sorption on WH biochars (BC300, BC450, BC600) at 30 °C

		Langmuir model			Freundlich model		
Pollutants	Biochars	q_{max} (mg g^{-1})	K_L (L mg^{-1})	R^2	K_F (L mg^{-1})	n	R^2
Cd	BC300	60.85	0.0249	0.98	14.09	4.453	0.75
	BC450	74.99	0.2786	0.98	37.38	8.093	0.78
	BC600	70.77	0.0712	0.98	26.47	6.239	0.71
Pb	BC300	119.58	0.0397	0.98	28.49	4.340	0.78
	BC450	128.95	0.1815	0.97	50.86	6.069	0.87
	BC600	123.37	0.1110	0.98	41.09	5.245	0.87

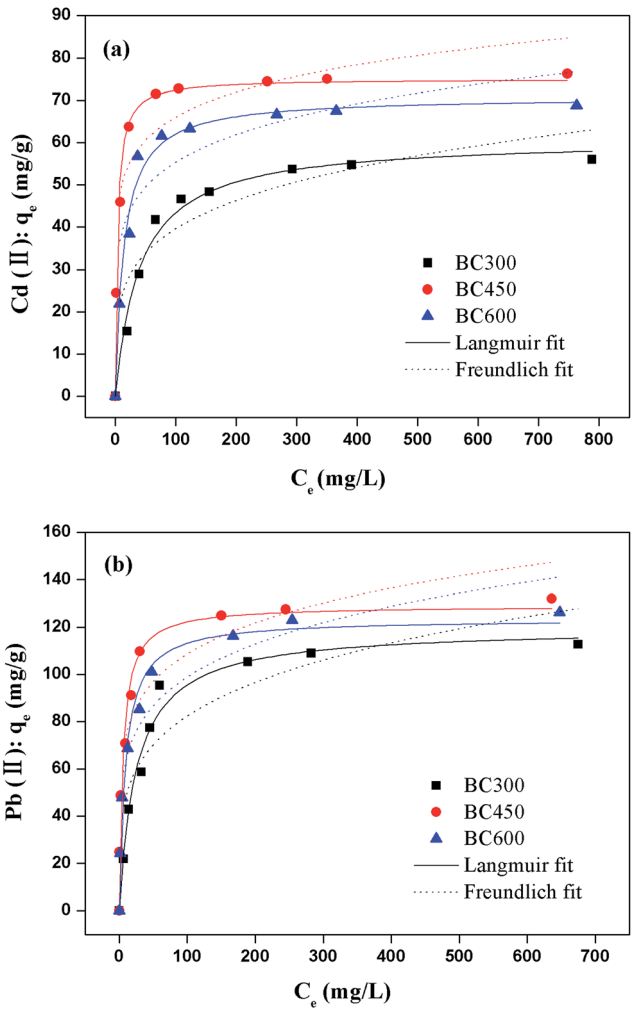

Fig. 7 Langmuir isotherm and Freundlich isotherm for the adsorption of Cd and Pb on biochars at 30 °C (solution volume: 50 mL; adsorbent dose: 0.1 g; contact time: 24 h; pH: 5.0).

3.5. Effect of pyrolysis temperature on biochars' adsorption

The physicochemical properties of biochar (porous structure, surface areas, element contents, cation exchange capacity and pH) are dependent on the pyrolytic temperature.[24,25] Ahmad, *et al.* demonstrated that biochar of higher pyrolytic temperature had higher hydrophobicity, surface area, pore volume, pore size together with low polarity that may have increased trichloroethylene adsorption from water.[26] Kim, *et al.* reported that pH and surface area of biochar increased greatly at pyrolytic temperature over 500 °C, resulting in the increase of Cd adsorption capacity with increasing pyrolytic temperature.[14]

In our study, BC450 showed the highest adsorption capacity, while BC300 had the lowest adsorption amount. This phenomenon could be explained by the following reasons: (1) the surface area of biochar increased and the porous structure of biochar developed with the increase of pyrolysis temperature,[27] which may contribute to the higher adsorption capacity; (2) there was a decrease of the amount of oxygen-containing functional groups (carboxyl, hydroxyl and ether) when pyrolysis temperature was increased. The disappearance of most oxygen-containing surface groups on BC600 would decrease heavy metals sorption onto biochar, though it had great surface area and porous structure. However, the porosity and functional groups of BC300 were incomplete, resulting in the lowest adsorption capacity comparing with BC450 and BC600. Therefore, the main mechanism for heavy metals adsorption was not the pore structure, but the reaction between heavy metals and surface functional groups.[28] These data calculated from isotherms process demonstrated that biochar properties were significantly influenced by pyrolysis temperatures, which played an important role in affecting adsorption characteristics.

3.6. Adsorption thermodynamic analysis

The thermodynamic data, such as Gibbs free energy ΔG^0, enthalpy ΔH^0, entropy ΔS^0, can be calculated using the following equations:

$$\Delta G^0 = -RT \ln K_e \quad (7)$$

$$\ln K_e = \frac{\Delta S^0}{R} - \frac{\Delta H^0}{RT} \quad (8)$$

where ΔG^0 is the stand free energy change of the ion exchange (kJ mol^{-1}), ΔH^0 (kJ mol^{-1}) is the enthalpy change, ΔS^0 (J mol^{-1} K^{-1}) is the entropy change, R is the universal gas constant (8.314 mol^{-1} K^{-1}), T is the absolute temperature (K), K_e is the thermodynamic equilibrium constant which was calculated by plotting $\ln(q_e C_e^{-1})$ *versus* q_e and extrapolating to zero q_e. The values of ΔH^0 and ΔS^0 can be determined from the intercept and slope of the linear plot of ΔG^0 *versus* T.

Thermodynamic parameters were shown in Table S2.† The negative values of ΔG^0 at three different temperatures indicated that the process of these adsorption were spontaneous in nature. Moreover, the values of ΔG^0 decreased with the increasing reaction temperature (25, 30, and 40 °C), which demonstrated that adsorption efficiency was higher in high temperature than that of in low temperature. The endothermic adsorption process was demonstrated by the positive value of ΔH^0 (Cd: 11.51 kJ mol^{-1}; Pb: 9.375 kJ mol^{-1}). Furthermore, the positive value of ΔS^0 presented the increasing randomness at the solution/solid interface during the adsorption. From these thermodynamic parameters, it can be concluded that these adsorption processes are spontaneous and endothermic.

3.7. Effect of background ionic strength on heavy metal removal

As shown in Fig. S2,† the NaCl had little influence on Cd^{2+} removal until the concentration of NaCl was 0.5 mol L^{-1}, and the removal capacity was reduced from 43.40 mg g^{-1} to 34.30 or 19.54 mg g^{-1} while the concentration of NaCl was 0.5 mol L^{-1} or 1 mol L^{-1}. However, the effect of NaCl on Pb^{2+} adsorption was more sensitive even at a relative low NaCl concentration (0.05 mol L^{-1}). The adsorption capacity of Pb^{2+} was 46.66 mg g^{-1} while no background ionic was dissolved, but the result dropped to 28.50 mg g^{-1} at 1 mol L^{-1} NaCl. The reason could be attributed to high concentrations of Cl^- and Na^+ which could hinder the electrostatic between the charges on biochar surface and heavy metals ions in solution. In addition, Cl^- and Na^+ could preempt surface adsorption sites of adsorbent before heavy metals ions react with biochar. Moreover, the high ionic strength of the solution could influence the activity coefficient of Cd^{2+} and Pb^{2+}, thus decreasing the collide and contact between the sorbent and solute.

3.8. Desorption studies

In order to analyze the desorption properties of water hyacinths biochar, desorption studies were conducted in 0.5 mol L^{-1} hydrochloric acid. Desorption efficiency were presented in Fig. S3,† it showed that the maximum desorption capacity of Pb^{2+} was 92.01% (95.46 mg g^{-1}) for BC450. Furthermore, the lowest desorption efficiency of Cd^{2+} was BC600, while that of Pb^{2+} was BC300, which could be assigned to the biochar' physicochemical properties, such as the specific surface area, pore volume and the functional group. Moreover, desorption efficiency of Pb^{2+} were higher than that of Cd^{2+}. These results indicated that WH biochar had a potential of regeneration for Cd^{2+} and Pb^{2+} adsorption.

3.9. Possible mechanisms for competitive adsorption of Cd and Pb

The mutual effects of coexisting Pb^{2+} and Cd^{2+} on adsorption of each other were evaluated and the results were shown in Fig. 8a and b. In comparison with the single system, the coexistence of Pb^{2+} and Cd^{2+} could influence the adsorption capacity each other, which demonstrated the competitive adsorption between Pb^{2+} and Cd^{2+}. Moreover, the effects of the coexistence of Pb^{2+}

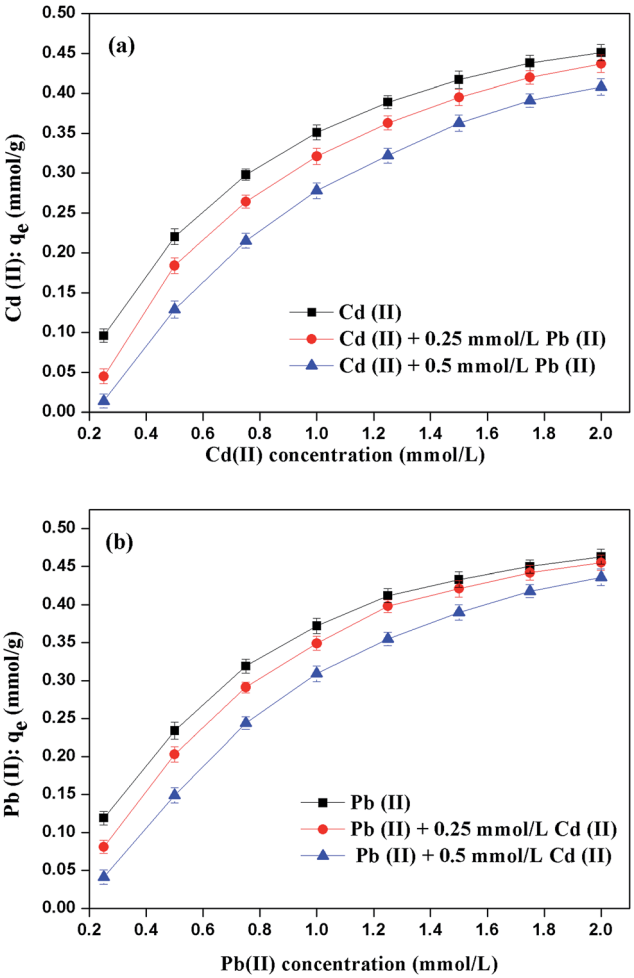

Fig. 8 (a) Effect of Pb(II) on Cd(II) adsorption by BC450 (solution volume: 50 mL; adsorbent dose: 0.1 g; contact time: 24 h; pH: 5.0; rpm: 140). (b) Effect of Cd(II) on Pb(II) adsorption by BC450 (solution volume: 50 mL; adsorbent dose: 0.1 g; contact time: 24 h; pH: 5.0; rpm: 140).

and Cd^{2+} at lower concentrations (0.25 mmol L^{-1}) decreased with the increase of adsorbents concentrations. While at higher concentrations (0.5 mmol L^{-1}), this phenomenon was not obvious. Furthermore, compared to the influence of Cd^{2+} on Pb^{2+} adsorption (Fig. 8b), the uptake of Cd^{2+} had a greater influence after Pb^{2+} addition (Fig. 8a). The difference suggested that the adsorption process in the mixture (Cd^{2+} and Pb^{2+}) was more favorable for Pb^{2+}. Therefore, a complexation interaction would probably occur in binary system.

Multiple mechanisms are involved in heavy metal sorption onto biochar, *e.g.*, ion exchange, electrostatic attraction, surface complexation, physical adsorption, co-precipitation, surface precipitation and innersphere complexation.[29–31] The schematic illustration of Cd and Pb sorption mechanisms was shown in Fig. 9. In our study, the FTIR spectra shown that the bands of oxygen-containing functional groups shifted marginally before and after adsorption, indicating carboxyl (–COOH) and/or hydroxyl (–OH) functional groups may be involved in coordination with Cd^{2+} and Pb^{2+} due to the complexation.[32]

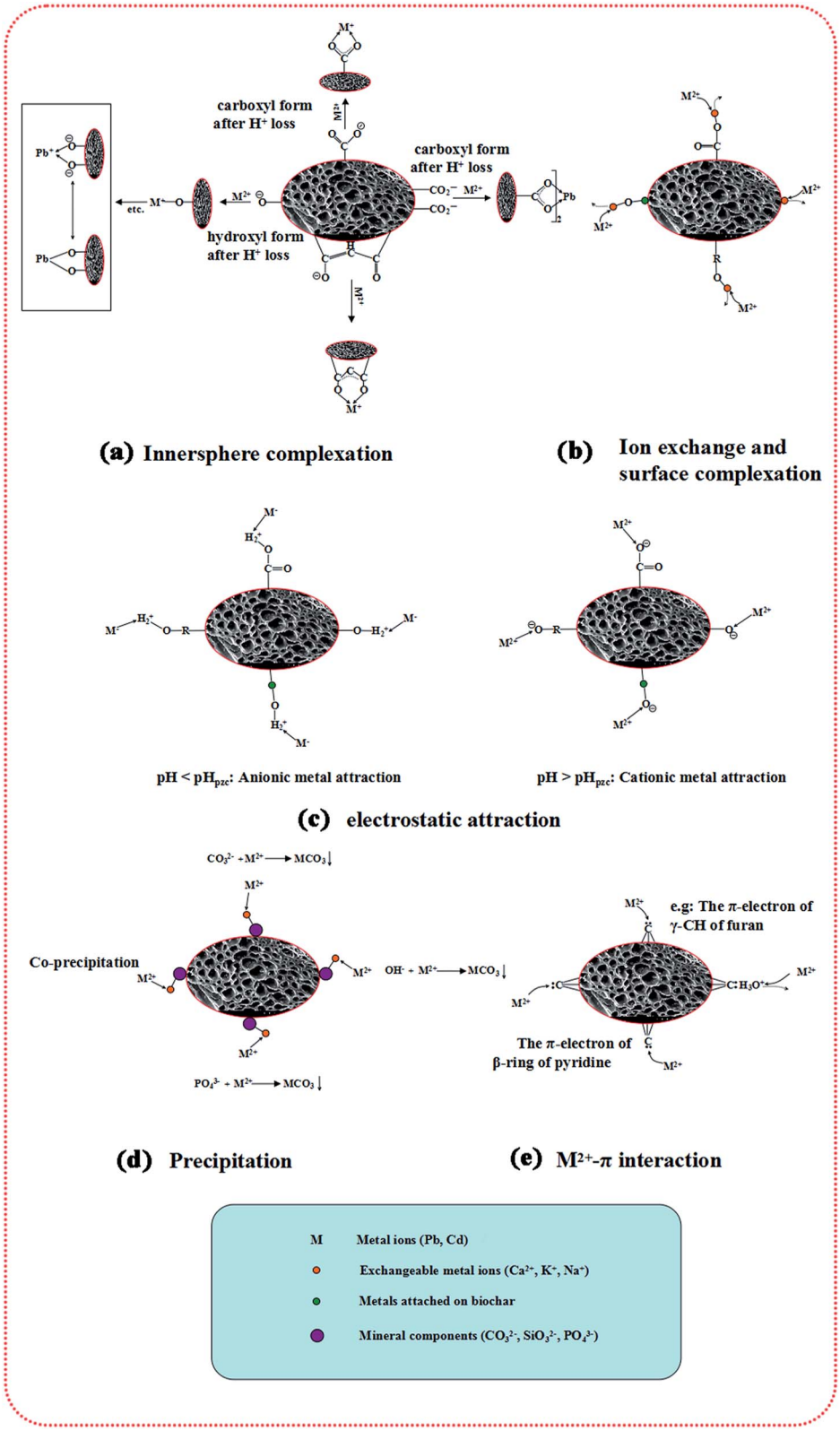

Fig. 9 The schematic illustration of Cd and Pb sorption mechanisms.

Furthermore, Cao, *et al.* demonstrated that the coordination between the oxygen-containing functional groups and heavy metals (*e.g.*, Cd^{2+} and Pb^{2+}) was usually accompanied with the release of H^+, resulting in the decrease of solution pH.[16] As presented in Fig. S4,† the solution pH of the blank system without heavy metals increased after biochar addition, resulting

Table 3 Net cations release from Cd or Pb sorption onto biochar BC450

Heavy metals	The net amount of metal cations released (mmol g^{-1})					Total heavy metals adsorbed (mmol g^{-1})
	$2K^+$	Ca^{2+}	$2Na^+$	Mg^{2+}	Total	
Pb	0.576	0.108	0.087	0.062	0.833	6.684
Cd	0.489	0.113	0.081	0.056	0.739	5.379

from the mineral ash from pyrolysis. However, the solution pH of the heavy metals sorption system decreased which compared to that of blank system.[33] Therefore, complexation may be one of the main adsorption mechanisms.

Moreover, before Pb and Cd adsorption, there is one peak in the O 1s spectrum at a binding energy about 532.7 eV. After Pb and Cd adsorption, a peak is observed at a binding energy greater than 532.4 eV. This indicated that some O atoms existed in a more oxidized state because of Pb or Cd adsorption. As a result of the formation complexes in reactions, in which a lone pair of electrons in the oxygen atom was donated to the shared bond between O and Pb or Cd, and then the electron cloud density of the oxygen atom was reduced, resulting in a lower binding energy peak observed.[34] Furthermore, the compound combined with the shared bond between Pb and O is more stable than that of formed between Cd and O, according to the linear relation of the cationic radii on the coordination number, as well as the relation between bond length and bond strengths for cation–oxygen bonds.[35] Therefore, these reasons may be mainly contributed to the competitive adsorption which was favorable for Pb^{2+}.

Considering the amount of Cd^{2+} and Pb^{2+} adsorbed on biochar increased with the increase of pH values (Fig. 5a), electrostatic attractions may play a significant role in sorption preferences. Furthermore, the amount of Pb^{2+} adsorbed on biochar was higher than Cd^{2+} at pH 2.0–5.0. The higher Pb^{2+} adsorption may be related to the larger size of the Pb^{2+} ion (Pb^{2+}: 1.32 Å; Cd^{2+}: 1.03 Å), which could induce the Pb^{2+} aquocation to simultaneously interaction electrostatically with a larger number of neighboring adsorption sites, thus stabilizing the adsorbed state.

The cyclic aromatic π-system could act as the π-donor to interact with heavy metal ions, which could serve as the π-acceptor due to their electron deficiency. As shown in Fig. 4, the weak band at 875.5 cm^{-1} was assigned to γ-CH of furan. The intensity of the peak at 875.5 cm^{-1} became weak after Pb adsorption, likely related to the bands of C=C stretching vibration in aromatic moieties,[32] while that of Cd loading became strong. However, the band at 875.5 cm^{-1} became strong after the mixture of Cd^{2+} and Pb^{2+} loading. According to the band changes in the heavy metal loading biochars, it can be concluded that cation–π interaction might be responsible for Cd^{2+} and Pb^{2+} sorption. The heterocyclic compound of γ-CH of furan was a weak cation–π binder, and may easily bind with Cd^{2+} compared with Pb^{2+} (binding energy: $Cd^{2+} < Pb^{2+}$).[36] These results showed that cation–π interaction was favorable for Cd^{2+}.

In addition, a new band at 684.6 cm^{-1} was observed after Pb^{2+} and the mixture sorption, which may present new Pb precipitates. Precipitation would occur between heavy metals and some ionized anions (*e.g.*, CO_3^{2-} and PO_4^{3-}) released from the minerals in biochars. Zhang, *et al.* reported that Cd precipitation as $CdCO_3$, $Cd_3(PO_4)_2$, and probably $Cd(OH)_2$ could be responsible for Cd adsorption on water hyacinths biochar produced at 450 °C,[37] which were consistent with the existence of CO_3^{2-} and P–O of phosphate analyzed by FTIR spectra. Moreover, compared to $Pb(OH)_2$, the precipitate formed between Cd^{2+} and OH^- was less soluble, according to the stability constants (pK_{sp}) ($Cd(OH)_2$: 14.28; $Pb(OH)_2$: 14.93). Similarly, the stability of $CdCO_3$ (pK_{sp}: 12.00) and $Cd_3(PO_4)_2$ (pK_{sp}: 32.60) were higher than that of $PbCO_3$ (pK_{sp}: 13.13) and $Pb_3(PO_4)_2$ (pK_{sp}: 42.10).[34] Therefore, it can be speculated that Cd^{2+} was prior to forming theses precipitates, which could inhibit Pb^{2+}sorption.

As shown in Table 3, cation exchange may be responsible for the reaction mechanisms of Cd^{2+} and Pb^{2+} removal. However, the contribution of cation exchange occupied a relatively small percentage in the total metals adsorbed. Moreover, the net amount of cations released from Pb^{2+} sorption onto biochar was higher than that of Cd^{2+} sorption onto biochar, indicating cation exchange was favorable for Pb^{2+}. The possible main reason may be that surface complexation between Cd or Pb and the oxygen groups is most likely through Cd or Pb exchange with the complexed cations contained in biochar (Fig. 9), and the complexing capacity of Pb is stronger than that of Cd.

Competitive adsorption may depend on such factors as ionic radius, ionic potential, chemical properties and hydrolysis state. The lower Pb^{2+} ionic charge/radius ratio (3.3) *versus* Cd^{2+} (1.9) leads to weaker Cd^{2+} ionic interaction forces *versus* Pb^{2+}, thus Pb^{2+} would be retained on more surface sites with weaker negative charge. In this study, the declined sorption capacity of Cd^{2+} in binary system were mainly attributed to the prior interactions between Pb^{2+} and oxygen-containing functional groups, and stronger complexing capacity of Pb^{2+}, as well as the prior electrostatic attractions between Pb^{2+} and surface adsorption sites with negative charge. However, the competition from the interactions of precipitate and cation–π should be responsible for the decrease of Pb^{2+} adsorption capacity. Therefore, these reasons may be contributed to the results in binary systems that the adsorption process was more favorable for Pb^{2+}.

4. Conclusion

This study proved that BC450 had the highest adsorption capacity for heavy metal compared to BC300 and BC600. Both in single and in binary system, Pb^{2+} had a higher amount of

adsorption on WH biochar compared with Cd^{2+}, and the coexistence of Pb^{2+} and Cd^{2+} could affect adsorption capacity of each other. Furthermore, the existence of Pb^{2+} inhibited the sorption of Cd^{2+}, which could be attributed to the complexation, cation exchange, and electrostatic attraction. However, the sorption of Pb^{2+} was affected by the existence of Cd^{2+}, which may result from the precipitate and cation–π interaction.

Acknowledgements

This study was financially supported by the National Natural Science Foundation and the Creative Research group of China (Grant no. 41271332, 51478470 and 51521006) and the Hunan Provincial Innovation Foundation For Postgraduate (Grant No. CX2015B090 and CX2015B095).

References

1 L. Wang, J. Zhang, R. Zhao, Y. Li, C. Li and C. Zhang, *Bioresour. Technol.*, 2010, **101**, 5808–5814.
2 D. Mohan, H. Kumar, A. Sarswat, M. Alexandre-Franco and C. U. Pittman, *Chem. Eng. J.*, 2014, **236**, 513–528.
3 W. Zhang, S. Mao, H. Chen, L. Huang and R. Qiu, *Bioresour. Technol.*, 2013, **147**, 545–552.
4 R. C. Brändli, G. D. Breedveld and G. Cornelissen, *Environ. Toxicol. Chem.*, 2009, **28**, 503–508.
5 M. Kobya, E. Demirbas, E. Senturk and M. Ince, *Bioresour. Technol.*, 2005, **96**, 1518–1521.
6 X. Cao, L. Ma, B. Gao and W. Harris, *Environ. Sci. Technol.*, 2009, **43**, 3285–3291.
7 H. Wang, K. Lin, Z. Hou, B. Richardson and J. Gan, *J. Soils Sediments*, 2010, **10**, 283–289.
8 M. Ahmad, S. S. Lee, X. Dou, D. Mohan, J. K. Sung, J. E. Yang and Y. S. Ok, *Bioresour. Technol.*, 2012, **118**, 536–544.
9 M. H. Duku, S. Gu and E. B. Hagan, *Sustainable Energy Rev.*, 2011, **15**, 3539–3551.
10 Y. Xue, B. Gao, Y. Yao, M. Inyang, M. Zhang, A. R. Zimmerman and K. S. Ro, *Chem. Eng. J.*, 2012, **200**, 673–680.
11 X. Dong, L. Q. Ma and Y. Li, *J. Hazard. Mater.*, 2011, **190**, 909–915.
12 C. Gan, Y. Liu, X. Tan, S. Wang, G. Zeng, B. Zheng, T. Li, Z. Jiang and W. Liu, *RSC Adv.*, 2015, **5**, 35107–35115.
13 X. Chen, G. Chen, L. Chen, Y. Chen, J. Lehmann, M. B. McBride and A. G. Hay, *Bioresour. Technol.*, 2011, **102**, 8877–8884.
14 W. K. Kim, T. Shim, Y. S. Kim, S. Hyun, C. Ryu, Y. K. Park and J. Jung, *Bioresour. Technol.*, 2013, **138**, 266–270.
15 G. Yang, L. Tang, G. Zeng, Y. Cai, J. Tang, Y. Pang, Y. Zhou, Y. Liu, J. Wang and S. Zhang, *Chem. Eng. J.*, 2015, **259**, 854–864.
16 X. Cao, L. Ma, B. Gao and W. Harris, *Environ. Sci. Technol.*, 2009, **43**, 3285–3291.
17 D. Mohan, C. U. Pittman, M. Bricka, F. Smith, B. Yancey, J. Mohammad, P. H. Steele, M. F. Alexandre-Franco, V. Gomez-Serrano and H. Gong, *J. Colloid Interface Sci.*, 2007, **310**, 57–73.
18 L. Tang, G. D. Yang, G. M. Zeng, Y. Cai, S. S. Li, Y. Y. Zhou, Y. Pang, Y. Y. Liu, Y. Zhang and B. Luna, *Chem. Eng. J.*, 2014, **239**, 114–122.
19 T. Y. Jiang, J. Jiang, R. K. Xu and Z. Li, *Chemosphere*, 2012, **89**, 249–256.
20 B. Wen, J. Zhang, S. Zhang, X. Shan, S. U. Khan and B. Xing, *Environ. Sci. Technol.*, 2007, **41**, 3165–3171.
21 M. Uchimiya, I. M. Lima, K. K. Thomas, S. Chang, L. H. Wartelle and J. E. Rodgers, *J. Agric. Food Chem.*, 2010, **58**, 5538–5544.
22 Y. S. Ho and G. McKay, *Process Biochem.*, 1999, **34**, 451–465.
23 D. Kołodyńska, R. Wnętrzak, J. Leahy, M. Hayes, W. Kwapiński and Z. Hubicki, *Chem. Eng. J.*, 2012, **197**, 295–305.
24 K. H. Kim, J. Y. Kim, T. S. Cho and J. W. Choi, *Bioresour. Technol.*, 2012, **118**, 158–162.
25 H. Yuan, T. Lu, D. Zhao, H. Huang, K. Noriyuki and Y. Chen, *J. Mater. Cycles Waste Manage.*, 2013, **15**, 357–361.
26 M. Ahmad, S. S. Lee, A. U. Rajapaksha, M. Vithanage, M. Zhang, J. S. Cho, S. E. Lee and Y. S. Ok, *Bioresour. Technol.*, 2013, **143**, 615–622.
27 P. Bonelli, E. Buonomo and A. Cukierman, *Energy Sources, Part A*, 2007, **29**, 731–740.
28 D. Sud, G. Mahajan and M. Kaur, *Bioresour. Technol.*, 2008, **99**, 6017–6027.
29 H. Lu, W. Zhang, Y. Yang, X. Huang, S. Wang and R. Qiu, *Water Res.*, 2012, **46**, 854–862.
30 X. Tan, Y. Liu, G. Zeng, X. Wang, X. Hu, Y. Gu and Z. Yang, *Chemosphere*, 2015, **125**, 70–85.
31 H. Zheng, Z. Wang, X. Deng, J. Zhao, Y. Luo, J. Novak, S. Herbert and B. Xing, *Bioresour. Technol.*, 2013c, **130**, 463–471.
32 Z. Wang, G. Liu, H. Zheng, F. Li, H. H. Ngo, W. Guo, C. Liu, L. Chen and B. Xing, *Bioresour. Technol.*, 2015, **177**, 308–317.
33 J. H. Yuan, R. K. Xu and H. Zhang, *Bioresour. Technol.*, 2011, **102**, 3488–3497.
34 L. Jin and R. Bai, *Langmuir*, 2002, **18**, 9765–9770.
35 J. Zio, *J. Solid State Chem.*, 1985, **57**, 269–290.
36 J. C. Ma and D. A. Dougherty, *Chem. Rev.*, 1997, **97**, 1303–1324.
37 F. Zhang, X. Wang, D. Yin, B. Peng, C. Tan, Y. Liu, X. Tan and S. Wu, *J. Environ. Manage.*, 2015, **153**, 68–73.

